

Substituting (A4) into (3.8b), we obtain

$$(\omega - \omega_I + i\epsilon)B(\omega) = \gamma^* \sum_p A_p(\omega) + |\beta|^2 (\omega - \omega_L + \frac{1}{2}i\Gamma_\lambda)^{-1} B(\omega). \quad (\text{A6})$$

Using (3.8a), we can solve for  $\sum_p A_p$ ;

$$\sum_p A_p(\omega) = \gamma B(\omega) \sum_p (\omega - \omega_p + i\epsilon)^{-1} + (iL)^{-1} \sum_p (\rho_0 - \rho - i\epsilon)^{-1} (\omega - \omega_p + i\epsilon)^{-1}. \quad (\text{A7})$$

The sums over  $p$  in (A7) can be performed similarly to

the derivation of (A2). The result is

$$\sum_p A_p(\omega) = -iL\gamma B(\omega) + (\omega - \rho_0 + 2i\epsilon)^{-1}. \quad (\text{A8})$$

Substituting (A8) into (A6), we can solve for  $B(\omega)$ ;

$$B(\omega) = \frac{\gamma^* (\omega - \omega_L + \frac{1}{2}i\Gamma_\lambda)}{(\omega - \rho_0 + 2i\epsilon) [(\omega - \omega_I + \frac{1}{2}i\Gamma_\gamma) (\omega - \omega_L + \frac{1}{2}i\Gamma_\lambda) - \beta^2]}, \quad (\text{A9})$$

where

$$\Gamma_\gamma = 2L|\gamma|^2. \quad (\text{A10})$$

Substituting (A9) into (3.8a), we obtain the desired expression for  $A(\omega)$ , (3.10).

## Resonant-Polaron-Coupling Investigation by a Study of Linewidths, Strengths, and Frequencies of Cyclotron Resonance and Magnetic-Impurity Absorption in InSb

C. J. SUMMERS,\* R. B. DENNIS, B. S. WHERRETT, P. G. HARPER, AND S. D. SMITH

*J. J. Thomson Physical Laboratory, University of Reading, Reading, England*

(Received 22 December 1967)

Detailed examination of the electron-phonon (polaron) coupling of optical lattice modes to the magnetic states of both conduction and donor electrons in InSb has been made in the Faraday configuration, where no plasma interaction is present. The striking discontinuity observed in linewidth as the cyclotron-resonance frequency ( $\omega_c$ ) passes through the longitudinal-optic-mode frequency ( $\omega_{LO}$ ) has been studied at temperatures of 15 and 88°K for donor concentrations from  $5 \times 10^{18}$  to  $1 \times 10^{16}$  cm<sup>-3</sup>. The smaller effect of a simultaneous shift in the frequency of magnetic absorption is also observed in this configuration. Similar effects are found for both conduction and bound electrons, and both are explained on the basis of a one-phonon-interaction model developed by Harper.

### INTRODUCTION

INTEREST in the electron-phonon interaction in polar crystals has been stimulated in the past two years by the application of magneto-optical techniques. These allow explicit study of the interaction of the electrons with the lattice longitudinal-optic modes. These modes are responsible for the mass change and energy shift predicted by Fröhlich's theory,<sup>1</sup> applicable to frequencies well removed from  $\omega_{LO}$ .

Before the measurements of Johnson and Larsen,<sup>2</sup> Dickey *et al.*,<sup>3</sup> and Summers *et al.*<sup>4</sup> the theoretical results were experimentally substantiated only by rather indirect measurements in highly polar materials.<sup>5,6</sup>

\* Present address: Bell Telephone Laboratories, Murray Hill, N. J.

<sup>1</sup> H. Fröhlich, *Advan. Phys.* **3**, 325 (1954).

<sup>2</sup> E. J. Johnson and D. M. Larsen, *Phys. Rev. Letters* **16**, 655 (1966); *J. Phys. Soc. Japan* **21**, 433 (1966).

<sup>3</sup> D. H. Dickey, E. J. Johnson, and D. M. Larsen, *Phys. Rev. Letters* **18**, 599 (1967).

<sup>4</sup> C. J. Summers, P. G. Harper, and S. D. Smith, *Solid State Commun.* **5**, 615 (1967).

<sup>5</sup> F. C. Brown, *Polarons and Excitons, Scottish Universities' Summer School, 1962* (Plenum Press, Inc., New York, 1963), p. 323.

<sup>6</sup> J. W. Hodby, J. A. Borders, F. C. Brown, and S. Foner, *Phys. Rev. Letters* **19**, 952 (1967).

The application of a magnetic field creates an electric dipole moment oscillating at the cyclotron frequency ( $\omega_c$ ) which may be swept through the frequency of the oscillatory polarization field produced by the longitudinal lattice modes.

We should distinguish between the "polaron," implying a quasiparticle as discussed by Fröhlich and others, referring to frequencies well removed from the active lattice mode frequency, and the resonant interaction studied here, which is, however, part of the same phenomenon. We shall use the term "polaron interaction" in this extended sense in this paper.

In indium antimonide the small effective mass makes the condition  $\omega_c > \omega_{LO}$  obtainable for moderate magnetic field strengths. In this material the Fröhlich coupling constant  $\alpha$  is small ( $\sim 0.02$ ). However, two effects have been observed: (1) a frequency shift<sup>3</sup> in the cyclotron-resonance absorption position, of the order of  $\omega_{LO}$ , as the cyclotron frequency is swept through  $\omega_{LO}$  and (2) a simultaneous discontinuity in the linewidth of the absorption,<sup>4</sup> which has definite structure.

As well as the quantum coupling of magnetic states to longitudinal lattice modes there may also be present

a dielectric coupling of the electronic and lattice polarizations. It has been noted by Summers *et al.*,<sup>4</sup> Kaplan *et al.*,<sup>7</sup> and confirmed experimentally by both, that in the Faraday configuration this dielectric coupling is absent. In the Voigt configuration, as used by Johnson and Larsen and Dickey *et al.*, it is present and its effects on the absorption may be obtained by a rotation transformation of the total dielectric tensor for the Faraday configuration, referring to the sum of the polaron polarization and lattice polarization. The advantage of the Faraday configuration, which avoids this complication, is evident.

The overlapping of impurity, spin up, and spin down Landau state absorptions complicates the measurements of linewidths. The relative population of these states is determined by temperature and impurity concentration. Therefore, in this paper we present a systematic study of the effects of these parameters on the nature, position, and linewidth of the magnetic absorptions in the region of the resonant electron-phonon interaction. A separation of effects has been made and we present new information on the interaction of impurity states and of the spin down Landau states with the longitudinal optic phonons.

The observed cyclotron absorptions are consistent with a theoretical complex dielectric constant  $\epsilon_+(\omega, B)$  [referring to right-hand circularly (r.h.c.) polarized light] based on a one-phonon coupling model (Harper<sup>8</sup>). Coupled electron-phonon eigenvalues used by Johnson and Larsen are obtained from  $\epsilon_+(\omega, B)$  by neglecting its imaginary component (which refers to broadening) and by solving for the poles  $\omega = \omega_c(B)$  of the remaining real component of  $\epsilon_+(\omega, B)$ . Both components are used here to explain the cyclotron frequency shift and the broadening. The results of the theory are summarized schematically for conduction electron states in Fig. 1.

The broad band of levels (indicated by the shaded strip) is due to coupling of the no-phonon,  $n=1$ ,  $\mathbf{k}$  states to the single,  $\mathbf{q}$ -phonon,  $n=0$ ,  $\mathbf{k}-\mathbf{q}$  states of the unperturbed energy  $\hbar\omega_{LO} + (\hbar^2/2m)(k_x - q_x)^2$ . The  $n=0$ , no-phonon  $\mathbf{k}$  states are unperturbed. The coupling removes the lattice degeneracies (neglecting dispersion) in  $q_x$  and  $q_y$ , and also the  $k_y - q_y$  Landau state degeneracy. Line broadening occurs as a consequence of decay of the no-phonon,  $n=1$ ,  $\mathbf{k}$  states into the one phonon,  $n=0$ ,  $\mathbf{k}-\mathbf{q}$  states of the same energy, with the emission of a phonon.

The nature of the *bound states* is discussed by various authors.<sup>9-11</sup> In the absence of a magnetic field, donor electron motion is, of course, localized to the impurity

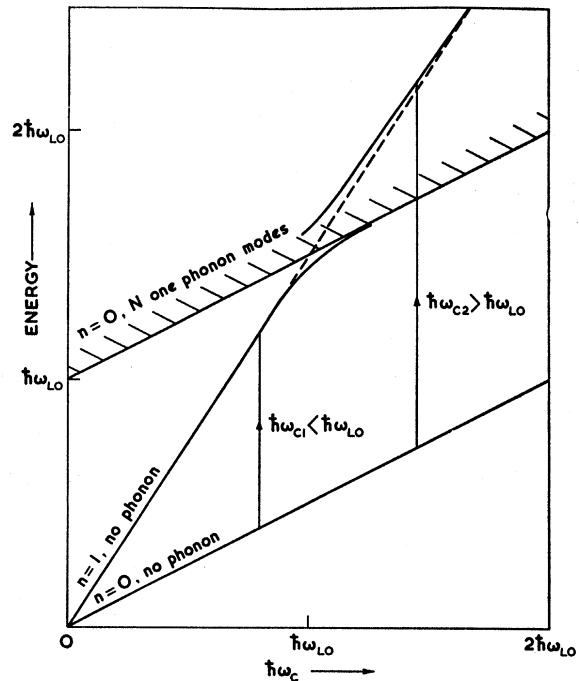


FIG. 1. Schematic representation of coupled electron-phonon energy levels as a function of magnetic field strength.

site by the Coulombic field of the ion. When a strong magnetic field is applied, such that the radius of the cyclotron orbit [ $R = (\hbar/2m\omega_c)^{1/2}$ ] is much smaller than the impurity Bohr radius ( $a_0 = 4\pi\epsilon\hbar^2/mde^2$ ), the donor electron motion perpendicular to the field is governed by the field. The motion in the direction of the field is still characterized by the Bohr radius, while conduction-electron motion is free in this direction.

Thus in the high field limit, the donor electron magnetic motion is seen to be similar to that of the conduction electrons. Selection rules for bound-state radiative transitions, implicitly quoted in the references above, are then expected to be the same as for Landau transitions. That is, in the Faraday configuration transitions from  $n=0$  to  $n=1$  states occur for r.h.c. polarized light for both bound and Landau states.

The impurity level system considered here is represented by single bound states below each Landau level (Fig. 2). For the present paper the Landau and bound states are treated as statistically independent and the previous electron-phonon coupling theory is extended to this case.

## EXPERIMENTAL DETAILS

Measurements of the cyclotron resonance absorption were made for indium antimonide samples with carrier concentrations varying from  $5 \times 10^{13}$  to  $1 \times 10^{15}$   $\text{cm}^{-3}$ . These details, together with the electrical mobilities and sample thicknesses, are given in Table I.

The magnetic field was generated by a superconduct-

<sup>7</sup> R. Kaplan, E. D. Palik, R. F. Wallis, S. Iwasa, E. Burstein, and Y. Sawada, *Phys. Rev. Letters* **18**, 159 (1967).

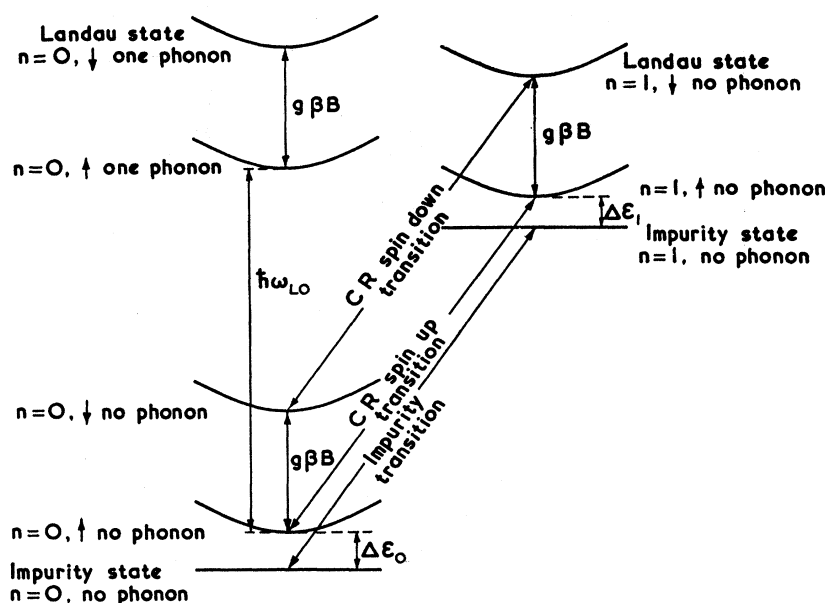
<sup>8</sup> P. G. Harper, *Proc. Phys. Soc. (London)* **92**, 793 (1967).

<sup>9</sup> Y. Yafet, R. W. Keyes, and E. N. Adams, *J. Phys. Chem. Solids* **1**, 137 (1956).

<sup>10</sup> R. E. Wallis and H. J. Bowlden, *J. Phys. Chem. Solids* **7**, 78 (1958).

<sup>11</sup> H. Hasegawa and R. E. Howard, *J. Phys. Chem. Solids* **21**, 179 (1961).

FIG. 2. The energy-level scheme, including spin and impurity states, showing the transitions considered.



ing, niobium-zirconium solenoid cooled to 4.2°K and capable of producing a maximum field of 66 kG. Specimens were positioned at the center of the solenoid and could be mounted in direct thermal contact with the parts of the cryostat system at either liquid helium, liquid nitrogen, or room temperature. Sample temperatures of  $15 \pm 5$  and  $88 \pm 3^\circ\text{K}$  were obtained consistently. The temperature was measured on the sample mount, using a gold (0.03% atomic iron)-chromel thermocouple. The propagation direction of radiation was along the axis of the solenoid, i.e., the system was in the Faraday configuration.

The transmission of unpolarized radiation through the sample was measured between 30 and 80  $\mu$  using a vacuum grating spectrometer. Data were taken at fixed photon energies while the field was swept up and down through the (near 200  $\text{cm}^{-1}$ ) resonance. The resolution of the spectrometer was one part in 120, and rejection of higher-order radiation better than one part in 500 was achieved by using transmission filters. The specimen thickness was a crucial factor in these experiments; perhaps surprisingly, the cyclotron resonance (CR) absorption for the carrier densities employed was high in comparison with the one-phonon, ionic lattice absorption, even quite close to the TO phonon frequency. Sample thickness was between 20 and 120  $\mu$  and meas-

urements could be made to within 5% of the TO frequency.

## RESULTS

As stated, the population factors for the  $n=0$  Landau level and its associated impurity level are strongly temperature-dependent for the conditions of our experiment. At 4.2°K the majority of the electrons are frozen in the impurity level for  $B > 10$  kG, resulting in the impurity absorption being stronger than the CR absorption (see, for example, Kaplan<sup>12</sup>). For slightly higher temperatures ( $\sim 15^\circ\text{K}$ ) more donors are ionized and the dominant absorption (Fig. 3 insets for 15°K, higher field peaks of the doublet) arises from CR spin up transitions. The  $n=0$  spin down state is not populated as this state, split by  $g\beta B$ , with  $g = -46.5$  is higher ( $\sim 5.1$  meV) than the Fermi energy ( $\sim 2.5$  meV) for the magnetic field strengths and carrier concentrations used.

At 88°K complete ionization has occurred and the absorption spectra show no sign of the impurity absorption. The increased thermal distribution of electrons now causes the  $n=0$  spin down magnetic state to be partially populated. This gives rise to CR absorption from the  $n=0$  to  $n=1$  spin down state (Fig. 3 insets for 88°K, again the higher field peak of the doublet). The relative strength of the spin down transition decreases with increase of magnetic field strength and increases with carrier concentration in the expected manner.

The magnetic field dependence of the position of both CR and impurity absorption peaks is shown in Fig. 3.

The energy offset ( $\sim 0.5$  meV) is clearly observed near the resonant polaron interaction position. The

TABLE I. Description of the samples used.

Carrier concentration ( $\text{cm}^{-3}$ )	Symbols used in figures	Thickness in microns	Electrical mobility at 77°K $\text{cm}^2/\text{V sec}$	Half-width for 25 kG	
				15°K	88°K
$5.7 \times 10^{13}$	$\Delta$	118	472 000	0.94	1.74
$1.13 \times 10^{14}$	$\circ$	82	474 000	0.78	1.31
$5.5 \times 10^{14}$	$+$	40	428 000	1.20	...
$1.0 \times 10^{15}$	$\square$	20	313 000	1.98	2.51

<sup>12</sup> R. Kaplan, J. Phys. Soc. Japan 21, 249 (1966).

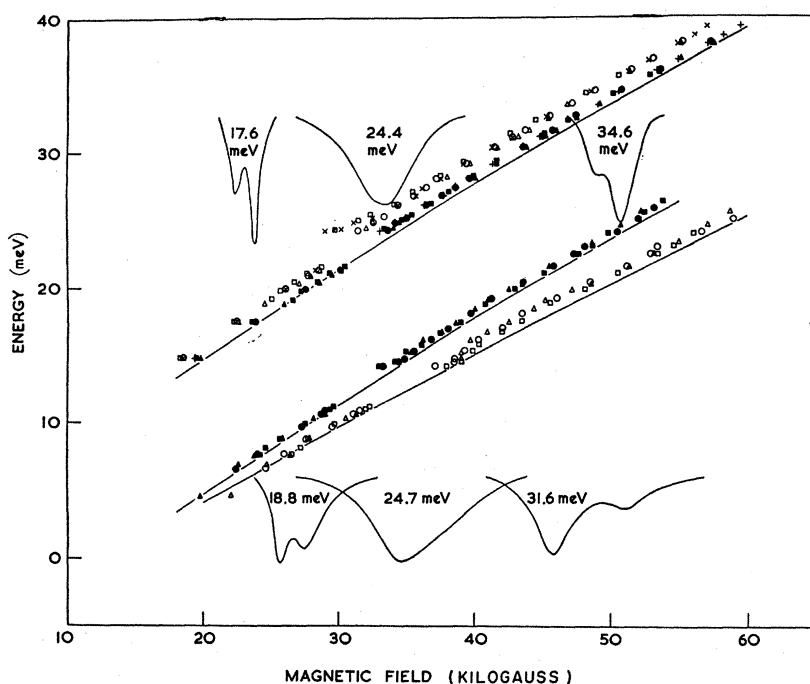


FIG. 3. Magnetic absorption energies as functions of magnetic field strength. The upper branch shows the spin up CR (solid points) and associated impurity transition energies (open points) for 15°K. The lower branch shows the spin up CR (solid points) and the spin down CR (open points) for 88°K. The insets show the transmission profiles as functions of magnetic field strength for various fixed photon energies at both temperatures. For identification of peaks see discussion of results (p. 759). For clear presentation, the 88°K results are shown 10 meV below their measured positions.

continuous lines shown in the figure give the theoretical energy dependence of the spin up and spin down CR transitions as computed by Pidgeon *et al.*,<sup>13</sup> (The theoretical shapes have been retained, but scaled to the experimental value of effective mass found here.)

The range of values of effective mass implied by the absorption frequencies of Fig. 3 are shown in Table II.

Although there have been at least 25 determinations of conduction electron masses in InSb since 1955,<sup>14</sup> nearly all experiments have given apparently different results. Even when properly reduced, for comparison, to the zero- $k$  zero-field mass  $m_0^*$ , values ranging from 0.0130 $m$ <sup>15</sup> to 0.0160 $m$ <sup>16</sup> have been quoted for 5°K. In view of the resolution of the transitions made possible by the ranges of carrier density and temperature em-

ployed in this work, we are able to clarify the situation from the present results.

Firstly, at both 15 and 88°K the variation of mass as a function of carrier density (i.e., band filling) from  $5 \times 10^{13}$  to  $1 \times 10^{15}$  cm<sup>-3</sup> is less than 1%, in agreement with  $k \cdot p$  theory.<sup>14,17</sup> Secondly, in this work, with clearly resolved lines, we have made a direct determination of the temperature dependence of conduction mass (at 15 and 88°K). As seen from Table II, the temperature variation is less than 1% between 15 and 88°K. This result is slightly surprising since from  $k \cdot p$  theory  $1/m_0^* \approx 4P^2/3E_G$ , where  $E_G$  is the energy gap, and  $P$  is the momentum matrix element. However, the recent determination of linear expansion coefficient for InSb by Novikova<sup>18</sup> shows a change of sign at 57.5°K and it is a coincidence that the lattice parameter is virtually unchanged at 15 and 88°K as a consequence. Our experimental results are therefore consistent with theory if only the dilational change<sup>19</sup> of  $E_G$  is concerned. This fact, also noted by Bell and Rogers,<sup>20</sup> is therefore directly confirmed.

The zero- $k$ , zero-field mass from these experiments is  $0.0137m \pm 0.0001m$ , in agreement with Dickey *et al.*<sup>3</sup> Thus with Bell and Rogers<sup>20</sup> reduction of Pidgeon's data<sup>21</sup> giving 0.0139 $m$ , interband and intraband methods

TABLE II. Effective masses deduced from absorption resonance frequencies (Fig. 3).

Field	15°K		88°K	
	Conduction electron mass	Impurity mass	Conduction electron mass	Spin split mass
20 kG	0.0152	0.0145	0.0153	0.0162
60 kG	0.0175	0.0171	0.0174	0.0193
Discontinuous change at $\omega_c = \omega_{LO}$	0.0006	0.0006	~0.0004	~0.0004

<sup>13</sup> C. R. Pidgeon, D. L. Mitchell, and R. N. Brown, Phys. Rev. **154**, 737 (1967).

<sup>14</sup> E. D. Palik and G. B. Wright, *Semiconductors and Semimetals* (Academic Press Inc., New York, 1967), p. 421.

<sup>15</sup> G. Dresselhaus, A. F. Kip, C. Kittel, and G. Wagoner, Phys. Rev. **98**, 556 (1956).

<sup>16</sup> B. Lax, J. G. Mavroides, H. J. Zeiger, and R. W. Keyes, Phys. Rev. **122**, 31 (1961).

<sup>17</sup> E. O. Kane, J. Phys. Chem. Solids **1**, 249 (1957).

<sup>18</sup> S. Novikova, Fiz. Tverd. Tela **2**, 2341 (1960) [English transl.: Soviet Phys.—Solid State **2**, 2087 (1961)].

<sup>19</sup> S. D. Smith, C. R. Pidgeon, and V. Prosser, in *Proceedings of the International Conference on Physics of Semiconductors, Exeter, 1962* (The Institute of Physics and The Physical Society, London, 1962), p. 301.

<sup>20</sup> R. L. Bell and K. T. Rogers, Phys. Rev. **152**, 746 (1966).

<sup>21</sup> C. R. Pidgeon and R. N. Brown, Bull. Am. Phys. Soc. **11**, 52 (1966); Phys. Rev. **146**, 575 (1966).

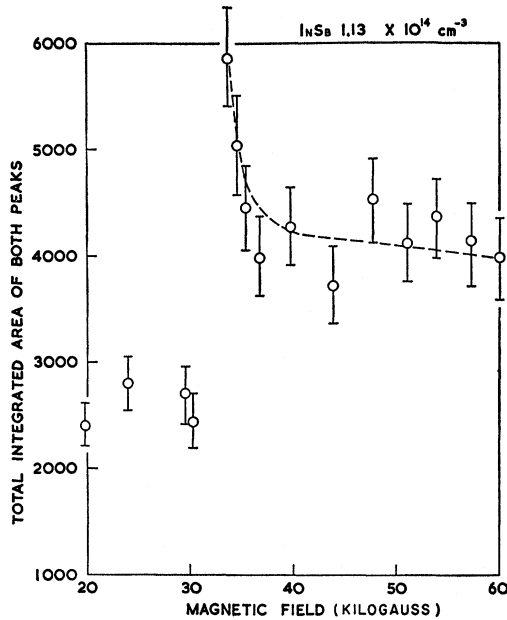


FIG. 4. Total integrated magnetic absorption as a function of magnetic field strength for the  $N=1.13 \times 10^{14} \text{ cm}^{-3}$  specimen at  $15^\circ\text{K}$ .

now give the same result within experimental error and not the 4% difference noted by Bell and Rogers.

The resolution of the absorption spectra into two peaks was done by assuming the dominant absorption peak to be symmetrical as a function of magnetic field. The difference between this and the total absorption spectrum was then attributed to the secondary feature; the linewidths of the two absorptions were calculated at half-height. The accuracy of the determination of the absorption peak position was  $\pm 0.2$  kG and the determination of linewidth varied from  $\pm 0.1$  to  $\pm 0.3$  kG, depending on whether the peaks were clearly defined or were in the strongly coupled region. Where measurements coincide, they agree well with those of Dickey *et al.*<sup>3</sup> and Kaplan.<sup>7</sup>

The broadening of the absorptions as  $\omega$  passes through  $\omega_{LO}$  is seen by reference to the insets of Fig. 3. The maximum strength of the absorption is only slightly affected above the coupling region. Figure 4 shows a significant discontinuity in the magnetic field dependence of the total integrated absorption of the system for the  $1.13 \times 10^{14} \text{ cm}^{-3}$  sample at  $15^\circ\text{K}$ .

This is unlike the behavior of free electron resonance but is consistent with the simple theory of the effect in that the density of states available for transitions is suddenly increased as the coupling region is reached so that the over-all absorption is increased. This result is obtained theoretically by an integration with respect to magnetic field of Eq. (2).

Figure 5(a) shows the abrupt change observed in the linewidth of the cyclotron resonance at  $15^\circ\text{K}$  as  $\omega$  passes through  $\omega_{LO}$ . This gross feature, first reported for a

carrier concentration of  $1.1 \times 10^{14} \text{ cm}^{-3}$ ,<sup>4</sup> was observed in all samples.

At  $88^\circ\text{K}$  the linewidth of the CR absorption [Fig. 5(b)] increases smoothly to approximately 1.5 times its value at 20 kG before the polaron interaction occurs. A sudden change is again observed for frequencies above  $\omega_{LO}$ . The field dependence of the linewidth above the critical coupling field decreases less rapidly at  $88^\circ\text{K}$  than at  $15^\circ\text{K}$ .

The residual half-widths at low fields are seen to increase in a consistent manner as the electrical mobility falls (Table I).

The linewidth dependence on magnetic field for the impurity transition [Fig. 5(c)] was analogous to the cyclotron absorption data, even exhibiting a similar dependence on electron mobility.

The spin down CR transition observed at  $88^\circ\text{K}$  also shows the effects of the polaron interaction in a similar manner but exhibits significantly wider lines throughout [Fig. 5(d)].

## THEORY AND DISCUSSION

The one-phonon interaction model of Harper gives the dielectric tensor element for r.h.c. polarized light as

$$\epsilon_+(\omega) = 1 - [\omega_p^2 / \omega Z(\omega)], \quad (1)$$

where  $\omega_p$  is the plasma frequency and  $Z(\omega)$ , analogous to complex impedance, contains the polaron coupling effects. The convention is used that the component of electric moment  $\mathbf{P}$  associated with r.h.c. polarized light is  $P_x + iP_y$ .

The cyclotron resonance absorption is proportional to the imaginary part of  $\epsilon_+$ .

$$\text{Im}\{\epsilon_+\} = \frac{\omega_p^2}{\omega} \text{Im}\left\{\frac{1}{Z(\omega)}\right\} = \frac{\omega_p^2}{\omega} \frac{Y(\omega)}{X^2(\omega) + Y^2(\omega)}, \quad (2)$$

where  $Z$  is expressed  $Z(\omega) = X(\omega) + iY(\omega)$ .

The absorption peak positions (i.e., the maxima of  $\text{Im}\{\epsilon_+\}$ ) are given approximately by the roots of  $X(\omega)$ ; the linewidths are given by values  $2Y(\omega)$ . Both  $X$  and  $Y$  are discontinuous as  $\omega$  passes through  $\omega_{LO}$ .

For  $\omega < \omega_{LO}$ ,  $Y(\omega) = 0$ .

$$X(\omega) = \omega - \omega_c - \alpha\omega_{LO} \left(\frac{\omega_{LO}}{\omega_c}\right)^{1/2} P \int_0^\infty x^3 \left(\frac{1}{x} - \frac{1}{a}\right) \frac{e^{-x^2}}{x^2 - a^2} dx,$$

where  $a^2 = (\omega_{LO} - \omega) / \omega_c$  and  $x$  is the variable of integration. For  $\omega > \omega_{LO}$ ,

$$Y(\omega) = \frac{1}{2} \alpha\omega_{LO} \left(\frac{\omega}{\omega_{LO}} - 1\right)^{-1/2} \int_0^\infty \frac{x e^{-x^2}}{x + [(\omega - \omega_{LO}) / \omega_c]} dx$$

and

$$X(\omega) = \omega - \omega_c - \alpha\omega_{LO} \left(\frac{\omega_{LO}}{\omega_c}\right)^{1/2} \int_0^\infty \frac{x^2 e^{-x^2}}{x^2 + [(\omega - \omega_{LO}) / \omega_c]} dx.$$

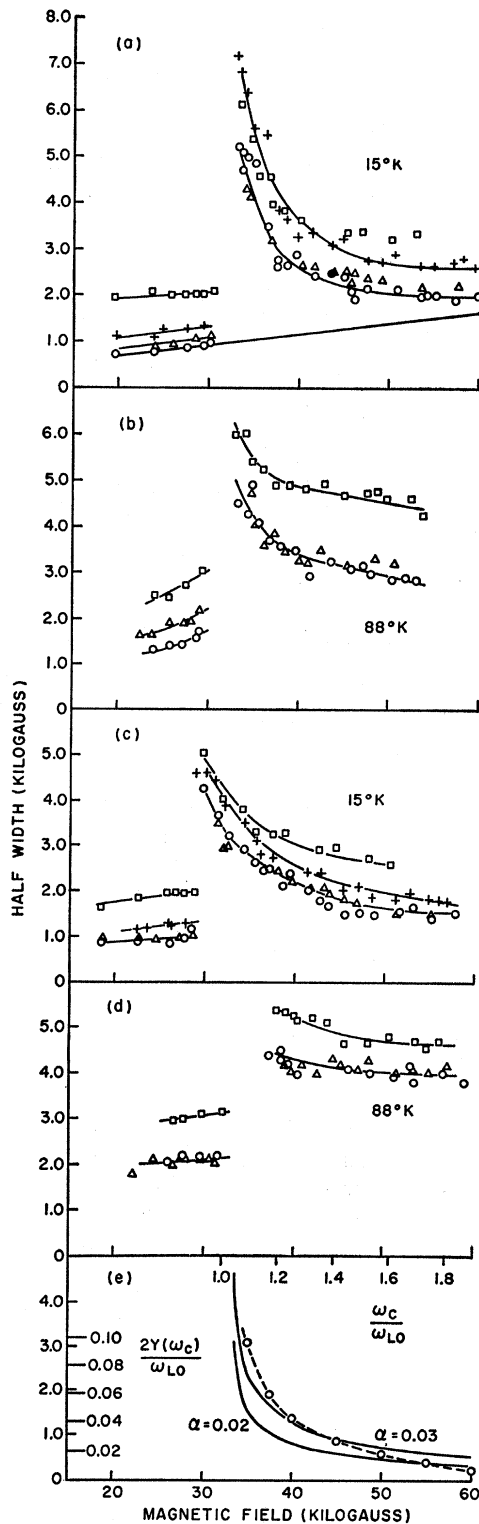


FIG. 5. Absorption linewidths for all specimens as functions of magnetic field strengths for (a) spin up cyclotron resonance at 15°K, (b) spin up cyclotron resonance at 88°K, (c) impurity absorption at 15°K, and (d) spin down cyclotron resonance at 88°K. (e) Comparison of theoretical and experimental polaron induced half-widths for the spin up CR absorption of the  $N=1.13 \times 10^{14} \text{ cm}^{-3}$  specimen at 15°K. By definition these are zero below the interaction region. For the key to the notation used see Table I.

Since  $Y(\omega)$  controls the linewidth, for  $\omega > \omega_{LO}$  the broadening due to polaron effects is characterized by the factor  $(\omega - \omega_{LO})^{-1/2}$ , the density of  $k_z$  levels in the  $n=0$ , one-phonon Landau state.

Figure 5(e) shows the comparison of theoretical and experimental linewidths. The experimental results were obtained by subtracting from linewidth values above  $\omega_{LO}$  a linear extrapolation of the low magnetic field data, i.e., assuming the total linewidth to be given by  $2\{[1/\tau(B)] + Y(\omega)\}$ , where  $\tau$  is the lifetime of electronic states in the absence of polaron coupling effects.

Calculation of theoretical linewidths was made using  $\omega_{LO} = 22.8 \text{ meV}$  (Picus *et al.*<sup>22</sup>) and  $\alpha = 0.020$ . The latter was calculated from the Fröhlich expression.

$$\alpha = \frac{1}{\sqrt{2}} e^2 \left( \frac{1}{\epsilon_\infty} - \frac{1}{\epsilon_0} \right) \left( \frac{m^*}{\omega_{LO} \hbar^2} \right)^{1/2},$$

using  $\omega_{LO} = 21.6 \text{ meV}$ ,  $\epsilon_\infty = 15.68$  (Picus *et al.*<sup>22</sup> and Hass and Hennis<sup>23</sup>). Comparison with the experimental results indicates a value for  $\alpha$  of  $0.025 \pm 0.005$ .

A computation of the roots of  $X(\omega)$  gives absorption frequencies of the same form as Dickey *et al.*,<sup>3</sup> in the interaction region but are without effects due to ground and higher Landau states ( $n > 1$ ) and two-phonon effects. The theoretical results are consistent with the experimentally determined energy offset within the limits of both experiment and theory, close to  $\omega_{LO}$ . In the limits of high and low frequencies,  $\omega \ll$  or  $\gg \omega_{LO}$ , our theory does *not* give the energy offset  $\alpha \hbar \omega_{LO}$ . In the region of the interaction we can express the frequency behavior in this weakly coupled case, in terms of change in effective mass (defined from  $\omega = eB/m^*$ ). The experimental values shift from  $0.0163m$  to  $0.0159m$ , a change of  $2\frac{1}{2}\%$ , between frequencies of  $\omega_{LO} \pm 5\%$ , in good agreement with a  $3\%$  change predicted by the theory (using  $\alpha = 0.02$ ) at these frequencies and  $5\%$  at  $\omega = \omega_{LO}$  itself. There are obvious objections to such a definition of effective mass in a resonantly coupled region.

Using the basis provided by Harper,<sup>8</sup> we shall now extend the polaron coupling theory to include the effects of bound impurity states associated with the  $n=0$  and  $n=1$  Landau levels. It has been shown that the same selection rules for the radiation polarization apply to Landau and impurity transitions.

The coupling of the two  $n=1$  levels to the  $n=0$ , one-phonon Landau continuum gives an explanation of the observed effects.

The one-phonon bound state associated with  $n=0$  degenerate Landau level has *no*  $k$  dependence and so does not present a continuum of states into which the  $n=1$  no-phonon state can decay, as required to explain experimental results. Its presence is therefore ignored.

Following Harper's notation,<sup>8</sup> independent wave functions for the Landau and impurity systems are given

<sup>22</sup> G. C. Picus, E. Burstein, B. W. Hennis, and M. Hass, *J. Phys. Chem. Solids* **8**, 282 (1959).

<sup>23</sup> M. Hass and B. W. Hennis, *J. Phys. Chem. Solids* **23**, 1099 (1962).

respectively, including their time dependence, by

$$\psi(\mathbf{k}, t) = \alpha_0(\mathbf{k}, t)\psi_{\mathbf{k},0}(t)\chi_0(t) + \alpha_1(\mathbf{k}, t)\psi_{\mathbf{k},1}(t)\chi_0(t) \\ + \sum_{\mathbf{q}} \beta(\mathbf{q}, \mathbf{k}, t)\psi_{\mathbf{k}-\mathbf{q},0}(t)\chi_{\mathbf{q}}(t)$$

and

$$\psi^I(t) = \alpha_0^I(t)\psi_0^I(t)\chi_0(t) + \alpha_1^I(t)\psi_1^I(t)\chi_0(t) \\ + \sum_{\mathbf{q}} \sum_{\mathbf{k}'} \beta^I(\mathbf{q}, \mathbf{k}', t)\psi_{\mathbf{k}',0}(t)\chi_{\mathbf{q}}(t),$$

where  $\alpha_0$ ,  $\alpha_1$ , and  $\beta$  are constants;  $\psi_{\mathbf{k},1}$  is the  $\mathbf{k}$ -electron wave function for the  $n=1$  Landau level and  $\chi_0$  and  $\chi_{\mathbf{q}}$  are, respectively, no-phonon and single  $\mathbf{q}$ -phonon wave functions. The superscript I indicates impurity level wave functions and state amplitudes. The sum over  $\mathbf{k}'$  is a consequence of the lack of  $\mathbf{k}$  dependence of the impurity states. There will be no  $\mathbf{k}$ -value selection rules for phonon coupling of such states with the one-phonon continuum states.

Under the experimental conditions reported, both the  $n=0$  bound and Landau states are populated. Initially, therefore,  $\alpha_0$  and  $\alpha_0^I$  are nonzero. In the independent scheme considered the ratio  $\alpha_0^2:\alpha_0^{I2}$  is given effectively by a Boltzmann distribution factor  $e^{-\Delta\epsilon_0/kT}$ , where  $\Delta\epsilon_0$  is the binding energy of the  $n=0$ , no-phonon impurity state (Fig. 2).

We now have the situation that for  $\omega_c < \omega_{LO}$  transitions are allowed between the sharp  $n=0$ , no-phonon and  $n=1$ , no-phonon Landau levels and between the  $n=0$  and  $n=1$  bound levels. As the magnetic field is increased the  $n=1$  Landau level passes into the  $n=0$ , one-phonon continuum and strong mixing occurs, with consequent broadening of the absorption peak. Furthermore, as the  $n=1$  bound state passes into the continuum, decay of the bound states into one-phonon Landau states of the same energy can also occur. Hence the impurity absorption peak is broadened in a similar manner to the Landau case. The broadening phenomena will occur at absorption frequencies  $\omega = \omega_{LO}$  (Landau) and  $\omega = \omega_{LO} + \Delta\epsilon_0/\hbar$  (impurity), respectively, with a simultaneous discontinuity in the absorption frequencies. The separation of the two absorption peaks for all magnetic fields is  $(\Delta\epsilon_0 - \Delta\epsilon_1)$ , where  $\Delta\epsilon_1$  is the  $n=1$  impurity binding energy (see Fig. 2).

The scheme of energy levels considered, and their coupling properties, is by no means a rigorous one. Radiation and phonon coupling between no-phonon bound and no-phonon Landau states is neglected, and also transitions to and from additional excited bound states are ignored for the present purpose. Radiation coupling between bound and Landau levels would result in two extra peaks at frequencies  $\omega_c - \Delta\epsilon_1/\hbar$  and  $\omega_c + \Delta\epsilon_0/\hbar$  and also at low frequency  $n=0$  bound to  $n=0$  Landau level transitions. Phonon-assisted coupling of  $n=0$ , no-phonon bound with  $n=1$  Landau states and  $n=0$ , no-phonon Landau with  $n=1$  bound states would modify all absorption peak strengths and positions to the order of the Fröhlich coupling constant  $\alpha$ . Such

couplings indicate radiative transitions from the  $n=0$  to the  $n=1$  states followed by coupling of the  $n=1$  bound and Landau states via decay into the  $n=0$ , one-phonon continuum. Finally, phonon coupling of the impurity and Landau  $n=0$ , no-phonon states would modify the state functions and the binding energy  $\Delta\epsilon_0$ .

Despite these qualifications, the simple scheme presented is believed to account for the primary phenomena.

The effects may be seen mathematically by following the procedures used by Harper, for the impurity-state wave function. For the present scheme the dipole moment  $\mathbf{P}_{total}$  for the complete system is the *sum* of Landau  $(\mathbf{P})^L$  and impurity  $(\mathbf{P})^I$  moments, taking into account the Boltzmann population factor.

$$\mathbf{P}_{total} \propto \{e^{-\Delta\epsilon_0/kT}\mathbf{P}^L + \mathbf{P}^I\}.$$

For r.h.c. polarized light, the associated Landau and impurity moments are given by

$$P_{+,L,I} = \frac{e^2}{m\omega} E_+ e^{-i\omega t} \{Z^{L,I}(\omega)\}^{-1}.$$

The complex impedance terms are

$$Z^L(\omega) = \omega - \omega_c - \hbar^{-2} \sum_{\mathbf{q}} \frac{\langle \psi_{\mathbf{k},1} | H_1 | \psi_{\mathbf{k}',0} \rangle^2}{\omega - \omega_{LO} + \epsilon_0 - \epsilon_0'}$$

and

$$Z^I(\omega) = \omega - (\omega_c + \Delta\epsilon_0 - \Delta\epsilon_1) \\ - \hbar^{-2} \sum_{\mathbf{q}} \sum_{\mathbf{k}'} \frac{\langle \psi_1^I | H_1 | \psi_{\mathbf{k}',0} \rangle^2}{\omega - \omega_{LO} + (\epsilon_0 - \Delta\epsilon_0) - \epsilon_0'},$$

where  $H_1$  is the Fröhlich electron-phonon coupling Hamiltonian. The width and strength of the impurity peak will thus depend on the matrix element  $\langle \psi_1^I | H_1 | \psi_{\mathbf{k}',0} \rangle$ .

The system considered is equivalent to the high magnetic field case with no-phonon coupling discussed by Hasegawa and Howard,<sup>11</sup> where only one bound state transition has appreciable oscillator strength. The separation of the observed peaks (1.05 meV at 40 kG, in agreement with Kaplan's photoconductivity experiments<sup>12</sup>) suggests that we are dealing experimentally with such a system, i.e., the second peak is *not* due to a bound state to Landau state transition, which has been predicted by Wallis and Bowlden<sup>10</sup> to have a separation from the CR absorption of approximately 3 meV ( $\Delta\epsilon_0$ ) at this field strength. Subsidiary peaks predicted by Hasegawa and Howard,<sup>11</sup> for the magnetic field strengths used, could not have been observed with the resolution available.

The frequency difference in the CR and impurity anomaly positions  $\Delta\epsilon_0$  was also not observable since  $\Delta\epsilon_0$  is less than 5% of  $\omega_{LO}$  and so lies in the region masked by the TO<sub>2</sub> absorption.

### CONCLUSIONS

Resonant polaron coupling effects between magnetic states and the longitudinal optic modes have been demonstrated for the longitudinal (Faraday) configuration where no plasma-coupling effects are expected. It is shown that linewidth and integrated absorption discontinuities are a more sensitive manifestation of the coupling than the energy offset or frequency deviation. A one-phonon interaction theory which includes calculation of the matrix elements of the transitions to the coupled states has been quantitatively compared with experiment. Good agreement of linewidth magnitudes is obtained and the polaron coupling constant is determined as  $\alpha = 0.025 \pm 0.005$  from the linewidth magnitudes. In the course of the experiment effects of free conduction electrons of both spin up and spin down levels and of bound impurity states are separated. Similar polaron coupling effects are observed for all three cases, and the theory is extended to the case of bound states, again in agreement with experiment.

The theory presented here for both free and bound states is intended to describe only the *resonant* coupling and is inadequate to give an accurate account of the differential polaron mass change between the  $B=0$  and  $B \rightarrow \infty$  limits. Indeed, our predicted mass difference between  $\omega_e < \omega_{LO}$  and  $\omega_e > \omega_{LO}$  tends to zero as  $B \rightarrow \infty$ . The theory presented by Dickey *et al.*<sup>3</sup> allows for shifts in the ground state level,  $n=0$ , as well as two-phonon processes (both neglected in the present work). While we believe that these corrections are small in the resonant coupling region, they will be relatively important for

$\omega_e \gg \omega_{LO}$  and will contribute to the high-field polaron mass. It should be noted, however, that energy levels alone [i.e., zeros of  $X(\omega)$ ] as given by Johnson, and Larson,<sup>2</sup> Dickey *et al.*<sup>3</sup>, and White and Koonce,<sup>24</sup> are insufficient in principle to determine mass parameters. The imaginary component  $Y(\omega)$ , as well as determining a lifetime, also contributes to the self-energy of the electron-hole pairs, though with decreasing effect for  $\omega_e \gg \omega_{LO}$ . Using this theory, we are able to predict the effects of phonon coupling on a variety of magneto-optic experiments, which depend on the components of the complex dielectric tensor, as given, for example, by Smith.<sup>25</sup>

An incidental result has been the determination of the impurity, temperature, and field dependence of conduction mass yielding a zero- $k$ , zero-field value of  $0.0137m \pm 0.0001m$ . This has clarified the divergence of results from previous experiments.

### ACKNOWLEDGMENTS

We wish to thank the Science Research Council of the United Kingdom for financial support for both experimental facilities and studentships (R.B.D. and B.S.W.). One of us (C.J.S.) wishes to thank the University of Reading for the award of a Research Fellowship during the tenure of which this work was done. We would also like to thank Miss C. M. Gregory for experimental and computational assistance.

<sup>24</sup> R. M. White and C. S. Koonce, *Phys. Rev. Letters* **17**, 436 (1966).

<sup>25</sup> S. D. Smith, *Handbuch der Physik* (Springer-Verlag, Berlin, 1967), Vol. 25, Chap. 2a, p. 234.